Kobe University Repository : Kernel

PDF issue: 2025-12-05

Quantum Transport Simulation of Silicon-Nanowire Transistors Based on Direct Solution Approach of the Wigner Transport Equation

Yamada, Yoshihiro
Tsuchiya, Hideaki
Ogawa, Matsuto

(Citation)
IEEE Transactions on Electron Devices,56(7):1396-1401

(Issue Date)
2009-07

(Resource Type)
journal article

(Version)
Version of Record

(URL)
https://hdl.handle.net/20.500.14094/90000909

KOBE UNIVERSITY

Quantum Transport Simulation of Silicon-Nanowire Transistors Based on Direct Solution Approach of the Wigner Transport Equation

Yoshihiro Yamada, Hideaki Tsuchiya, *Senior Member, IEEE*, and Matsuto Ogawa, *Member, IEEE*

***Abstract*—In this paper, we present a self-consistent and 3-D quantum simulator for Si-nanowire transistors based on the Wigner function model and multidimensional Schrödinger–Poisson algorithm. To achieve a sufficient numerical accuracy for calculating subthreshold current, we introduced a third-order differencing scheme for discretizing the drift term in the Wigner transport equation. By comparing with semiclassical Boltzmann and nonequilibrim Green's function approaches, the validity of the present simulator is confirmed. We also demonstrate that the source–drain tunneling is a critical physical phenomenon related to a scaling limit of nanowire devices, and the semiclassical simulation measurably underestimates a minimum gate length.**

***Index Terms*—Boltzmann transport equation, gate-all-around (GAA) configuration, nonequilibrium Green's function (NEGF) method, quantum confinement, silicon-nanowire transistors (SNWTs), source–drain (S-D) tunneling, subthreshold swing (SS), Wigner transport equation.**

I. Introduction

SILICON-NANOWIRE transistors (SNWTs) are promising candidates as extremely downscaled MOSFETs for the future Si-VLSIs, because device structures with gate-all-around (GAA) configurations provide better electrostatic gate control than the conventional planar structures, and a higher current capability due to an improved electronic bandstructure is expected [1]. To understand the device physics of SNWTs and assess their performance limits, quantum-transport simulator considering 3-D electrostatic gate control, atomistic effects, and realistic scattering processes is required. Recently, a number of computational studies on electrical properties of SNWTs have been reported [2]–[4], but they are based on the semiclassical Boltzmann transport equation which disregards quantum-mechanical transport of carriers along the source–drain (S-D) direction, although the 2-D quantum confinement in its cross section is considered by solving the 2-D Schrödinger equation. Therefore, such semiclassical computational approaches are only applicable for decananometer-scaled SNWTs with channel lengths longer than 10 nm [2]–[4]. However, SNWTs are expected to be practically used as a high-performance elemental device in sub-10 nm regime, so precise consideration of quantum transport of carriers is indispensable [5].

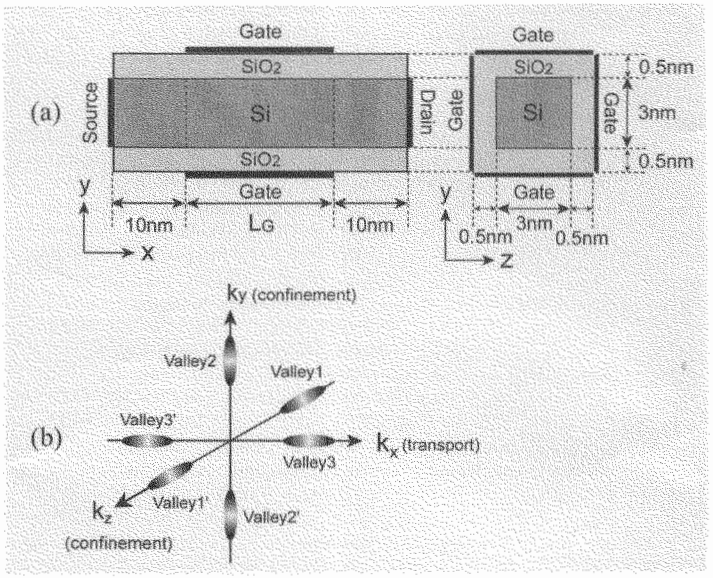

Fig. 1. (a) GAA-SNWT device model and (b) conduction-band valleys of Si.

In this paper, we present a 3-D quantum simulator based on a direct solution of the Wigner transport equation [6], [7], coupled with multidimensional Schrödinger–Poisson algorithm. The Wigner transport equation is a quantum–mechanical carrier transport equation that fully considers quantum–mechanical effects. In particular, we introduced a third-order differencing scheme (TDS) for discretizing the drift term in the Wigner transport equation, to achieve a sufficient numerical accuracy in the subthreshold region. The present quantum simulator can handle all quantum effects in SNWTs, such as 2-D quantum confinement and S-D tunneling, where the significance of S-D tunneling is verified by comparing with a semiclassical Boltzmann approach. Furthermore, the subthreshold swings (SSs) are compared with the results from the nonequilibrium Green's function (NEGF) method [8], and its validity and a scaling limit are discussed.

II. Computational Method

A. Model and Theory

The SNWT device model used in this paper is shown in Fig. 1(a), where GAA structure is employed, and its cross

Manuscript received December 5, 2008; revised April 3, 2009. Current version published June 19, 2009. This work was supported by the Semiconductor Technology Academic Research Center (STARC). The review of this paper was arranged by Editor M. Reed.

The authors are with the Department of Electrical and Electronics Engineering, Graduate School of Engineering, Kobe University, Kobe 657-8501, Japan (e-mail: tsuchiya@eedept.kobe-u.ac.jp).

Color versions of one or more of the figures in this paper are available online at http://ieeexplore.ieee.org.

Digital Object Identifier 10.1109/TED.2009.2021355

0018-9383/$25.00 © 2009 IEEE

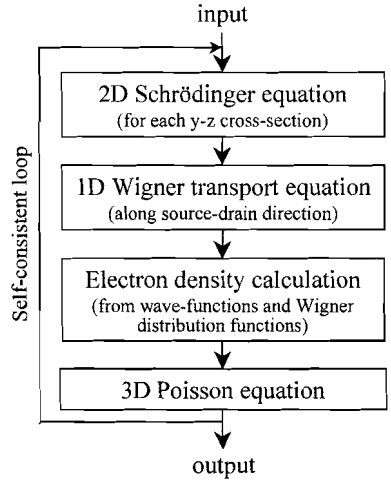

Fig. 2. Computational algorithm based on Wigner function model.

section is 3 nm × 3 nm with the gate oxide thickness of 0.5 nm. The donor concentration in the source and drain regions is 10^{20} cm^{-3}, and the channel region is undoped. The conduction-band valleys of Si is shown in Fig. 1(b), where the channel direction is taken as ⟨100⟩ and the confinement directions ⟨010⟩ and ⟨001⟩ for simplicity. To simulate quantum transport in such nanowire devices, we have developed a computational algorithm based on the Wigner transport formalism, as shown in Fig. 2. In this approach, the 3-D Wigner transport equation is decoupled into the 1-D Wigner transport equation along the S-D (x) direction and the 2-D Schrödinger equation in the transverse (y, z) cross section. Then, Wigner distribution function is defined for each quantized subband n for the three pairs of the conduction-band valleys, $v = 1{-}1'$, $2{-}2'$, and $3{-}3'$. This so-called mode-space approximation is considered to be valid for uniform nanowire devices used in this paper. The formation of uncoupled quantized subbands is computed by solving the 2-D Schrödinger equations for each $y{-}z$ cross section and each conduction-band valley with the anisotropic effective masses of conduction band, where the vanishing wave functions at the Si/SiO_2 interfaces are assumed. We applied the Lanczos method based on the modified Gram–Schmidt orthogonalization to solve the 2-D Schrödinger equations. Next, by using the obtained subband profiles $E_n^\nu(x)$, the 1-D Wigner transport equation at steady state given in (1) is solved along the S-D direction

$$\frac{\hbar k}{m_v^*}\frac{\partial f^{n,v}}{\partial \chi} + \frac{1}{\hbar}\int \frac{dk'}{2\pi} V^{n,v}(\chi, k-k') f^{n,v}(\chi, k') = \left(\frac{\partial f}{\partial t}\right)_C \tag{1}$$

where $V^{n,v}(\chi, k)$ is the nonlocal potential term given by

$$V^{n,v}(\chi, k) = 2\int_0^\infty d\xi \sin(k\xi)\left[E_n^\nu\left(\chi+\frac{\xi}{2}\right) - E_n^\nu\left(\chi-\frac{\xi}{2}\right)\right]. \tag{2}$$

This term represents quantum–mechanical effects such as tunneling. Note that χ and ξ denote the diagonal and cross-diagonal coordinates between space variables x and x', respectively; $\chi = (x + x')/2$, and $\xi = x - x'$. Furthermore, it is well known that the Wigner transport equation (1) reduces to the semiclassical Boltzmann transport equation in the limit of $\hbar \to 0$ [6], [7].

The right-hand side of (1) stands for collisional term. For phonon scatterings, the collisional term can be represented by using a scattering integral similar to that in the Boltzmann transport equation [9], which includes distribution functions of carriers in different valleys and subbands, and can further involve quantum features such as collisional broadening. A discussion on the rigorous inclusion of scattering in the Wigner approach can also be found in [10]. In this paper, however, we employed a simplified relaxation-time approximation (RTA) as a first step to consider scattering effects with moderate computational resources, as given by [11]–[13]

$$\left(\frac{\partial f}{\partial t}\right)_C \approx -\frac{1}{\tau}\left[f^{n,v}(\chi,k) - \frac{f_{eq}^{n,v}(\chi,k)}{\int dk f_{eq}^{n,v}(\chi,k)}\int dk' f^{n,v}(\chi,k')\right] \tag{3}$$

where τ and $f_{eq}^{n,\nu}$ denote the relaxation time and the distribution functions at equilibrium state, respectively. In this paper, note that $f_{eq}^{n,\nu}$ was substituted by equilibrium Wigner distribution functions actually computed at $V_D = 0$ V, not the analytical Fermi–Dirac function. We add that (3) ensures charge conservation, while intersubband scattering is not considered. In an ultrasmall nanowire, the intersubband scattering will not play a major role, because the minimum energies of the subbands are well separated by quantization. The value of τ was calculated by using the mobility of 500 cm^2/(V · s) and the relation of $\tau_\nu = m_\nu^* \mu / e$ for each conduction-band valley, since the mobility is a more familiar parameter than the relaxation time.

To analyze the gate control in SNWTs, the 3-D Poisson equation is self-consistently solved by using the preconditioned conjugate-gradient method with the incomplete Cholesky factorization. Since the main purpose of this paper is to demonstrate the validity of the present Wigner approach, we introduced the effective mass approximation and RTA. However, the present approach is applicable for atomistic simulation beyond the effective mass approximation and can include physics-based scattering processes [9]. Such extensions are currently in progress.

B. Discretization Method

As is well known, numerical solutions of the Wigner function model significantly depend on discretization methods for solving (1) and (2). Frensley [11] pointed out that discrete Wigner function is not generally consistent with discrete density operator, and thus, some of the information contained in the density operator will be lost in the Wigner function, because the (χ, ξ) mesh points are only half as dense as the (x, x') mesh points. A way to incorporate all the (x, x') points might be to use a staggered mesh in (χ, ξ) with mesh spacing of $\Delta_\chi = (1/2)\Delta_x$ and $\Delta_\xi = 2\Delta_x$. Mains and Haddad [14] have investigated such a scheme on the potential term of (2), but it seems to be only applicable for equilibrium situation due to the requirement for

central differencing scheme (CDS) to be employed. Therefore, we adopted in this paper a simpler alternative approach to provide higher numerical accuracy as proposed by Buot and Jensen [12], which introduces higher order differencing scheme for the spatial-derivative term on the left-hand side of (1). We expect that such a simpler modification will be effective in the present nano-MOS simulation.

In this paper, we examined three types of differencing schemes, which are first-order differencing scheme (FDS) [6], [7], [11]

$$\left.\frac{\partial f}{\partial \chi}\right|_{\mathrm{FDS}} = \frac{\mp f(\chi) \pm f(\chi \pm \Delta_\chi)}{\Delta_\chi} \tag{4}$$

second-order differencing scheme (SDS) [12]

$$\left.\frac{\partial f}{\partial \chi}\right|_{\mathrm{SDS}} = \frac{\mp 3f(\chi) \pm 4f(\chi \pm \Delta_\chi) \mp f(\chi \pm 2\Delta_\chi)}{2\Delta_\chi} \tag{5}$$

and TDS

$$\left.\frac{\partial f}{\partial \chi}\right|_{\mathrm{TDS}} = \frac{\mp 2f(\chi \mp \Delta_\chi) \mp 3f(\chi) \pm 6f(\chi \pm \Delta_\chi) \mp f(\chi \pm 2\Delta_\chi)}{6\Delta_\chi} \tag{6}$$

where the upper and lower signs correspond to upwind ($k_x < 0$) and downwind ($k_x > 0$) schemes, respectively. We believe that this is the first time to practically apply TDS to solve the Wigner transport equation (1). It can be readily proven that TDS corresponds to a hybrid scheme consisting of CDS and SDS with combination ratio of 2 : 1 as follows:

$$\left.\frac{\partial f}{\partial \chi}\right|_{\mathrm{TDS}} = \frac{2}{3}\frac{f(\chi+\Delta_\chi) - f(\chi-\Delta_\chi)}{2\Delta_\chi}(\mathrm{CDS}) + \frac{1}{3}\frac{\mp 3f(\chi) \pm 4f(\chi \pm \Delta_\chi) \mp f(\chi \pm 2\Delta_\chi)}{2\Delta_\chi}(\mathrm{SDS}). \tag{7}$$

Therefore, TDS may possibly be linked to the Mains and Haddad's idea mentioned earlier, which is worthy of consideration for further improvement in numerical accuracy and stability of the Wigner function model.

The conventional boundary conditions for the Wigner transport equation [6] are used in the simulation, i.e., the equilibrium Fermi–Dirac functions are imposed for electrons injected into a device region, while distribution functions for outgoing electrons are determined by solutions of (1). Such boundary conditions should be used at contacts sufficiently away from a quantum region, because electron transport in reservoirs attached to the device is supposed to be classical.

III. Results

A. Higher Order Differencing Schemes

First, Fig. 3 shows the I_D–V_G characteristics computed by applying FDS, SDS, and TDS to the whole device region. First, for the FDS approach, unexpectedly large subthreshold current is observed below $V_G = 0.2$ V. SDS significantly improves such a subthreshold-current behavior, but it occasionally outputs negative subthreshold current at small gate biases. TDS further improves the subthreshold-current behavior and allows us to estimate the SSs as presented later. On the other hand, the on-currents at large V_G conditions are almost independent of the differencing schemes. Therefore, careful treatment of differencing scheme is needed for a precise simulation in the subthreshold region. As for computational time, both SDS and TDS require CPU time about twice as large as FDS. Hereafter, we will use TDS in the Wigner approach.

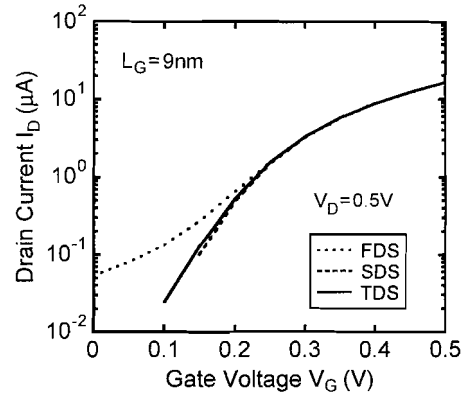

Fig. 3. I_D–V_G characteristics computed by using FDS, SDS, and TDS for the spatial-derivative term in the Wigner transport equation. $L_G = 9$ nm and $V_D = 0.5$ V.

B. Multisubband Quantum Transport

Next, we present multisubband quantum transport of SNWTs. Fig. 4(a) shows the subband profiles and Fig. 4(b) the electron-density profiles for several quantized subbands along the S-D direction, where $L_G = 6$ nm, $V_D = 0.5$ V, and $V_G = 0.25$ V. The valleys $1-1'$ and $2-2'$ are completely degenerated because of the square cross section. These four valleys have the larger confinement effective mass (m_l) in the y- or z-direction, so their lowest ($n = 1$) and first higher ($n = 2$) subbands are located below the lowest subband of the valleys $3-3'$ ($n' = 1$), as shown in Fig. 4(a). As a result, most of the electrons are populated in those four valleys, as shown in Fig. 4(b). This is favorable from the point of view of drive current, because they have the smaller transport effective mass of m_t.

Next, Fig. 5 shows the variations in the total electron-density profiles due to gate-bias voltage for the gate lengths of 9 [Fig. 5(a)] and 6 nm [Fig. 5(b)]. Note that each profile is compared with that from a semiclassical Boltzmann approach where the 1-D Boltzmann transport equation is solved along the S-D direction, while the 2-D Schrödinger equations are solved in the same manner as mentioned in Section II-A. For $L_G = 9$ nm, a significant difference between the Wigner and Boltzmann approaches is not observed for all gate biases, as shown in Fig. 5(a). On the other hand, when the gate length reduces to 6 nm, the electron densities in the channel are found to be larger for the Wigner approach, particularly at smaller gate biases, as shown in Fig. 5(b). This is due to S-D tunneling of conduction-band electrons discussed later again.

Fig. 6 shows the Wigner and Boltzmann distribution functions computed at $V_G = 0.2$ V (subthreshold) [Fig. 6(a)] and

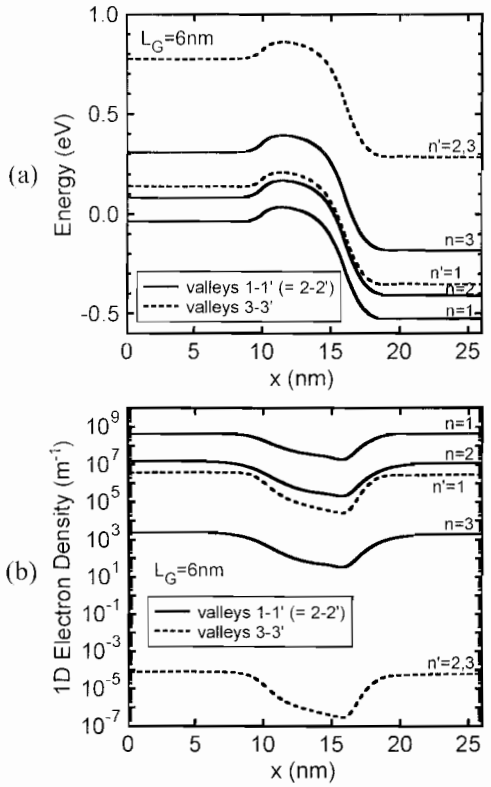

Fig. 4. (a) Subband profiles and (b) electron-density profiles for several quantized subbands along S-D direction. $L_G = 6$ nm, $V_D = 0.5$ V, and $V_G = 0.25$ V.

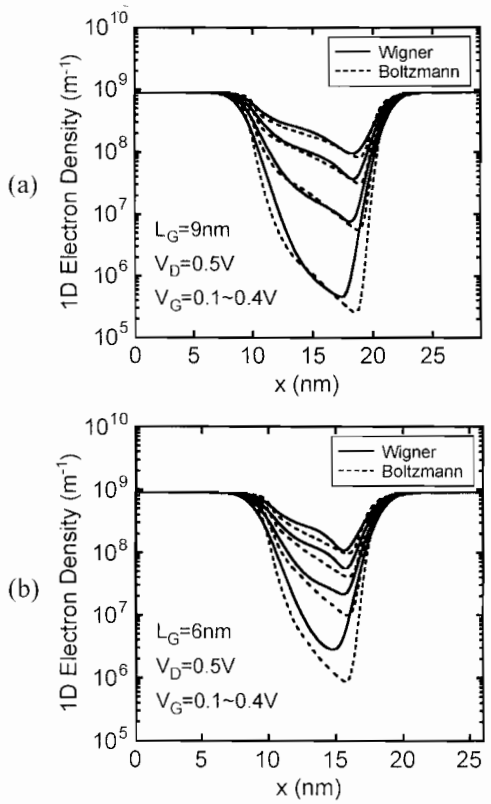

Fig. 5. Variations in total electron-density profiles due to gate-bias voltage for (a) $L_G = 9$ nm and (b) $L_G = 6$ nm. Results from the semiclassical Botzmann approach are also plotted in the dashed lines.

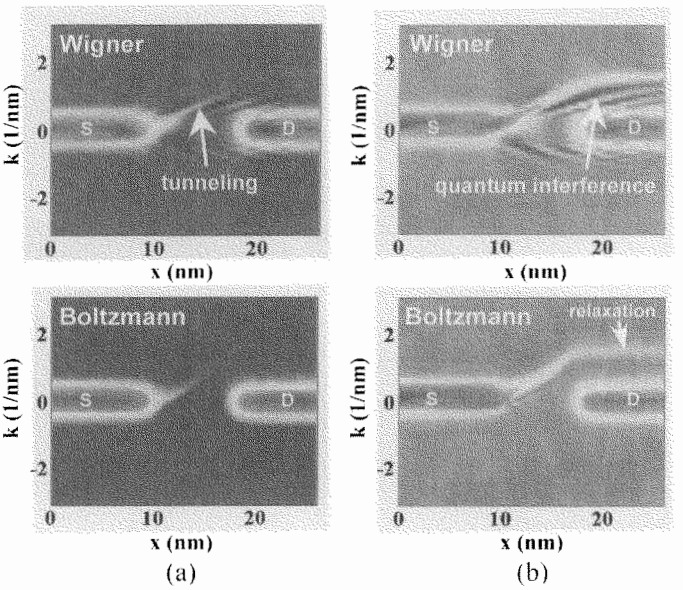

Fig. 6. Wigner and Boltzmann distribution functions computed for (a) $V_G = 0.2$ V (subthreshold) and (b) $V_G = 0.4$ V (ON-state), for the lowest subband. $L_G = 6$ nm and $V_D = 0.5$ V. Color (gray) scale is different between (a) and (b) in order to emphasize the tunneling behavior observed in the Wigner result of (a).

0.4 V (ON-state) [Fig. 6(b)], for the lowest subband. First, at the subthreshold region, as shown in Fig. 6(a), tunneling electron waves from source to drain are found in the result of the Wigner distribution function, and in addition, the dark areas observed in the source and drain regions denote carrier accumulation due to quantum repulsion from the spatially varying channel potential. At the ON-state, as shown in Fig. 6(b), quantum interference pattern appears in the Wigner distribution function, which is particularly emphasized in the drain region. On the other hand, hot-electron relaxation happens in the drain electrode as found in the Boltzmann distribution function of Fig. 6(b), but it is not sufficiently thermalized. This suggests that a longer drain region or realistic phase-randomizing process, instead of RTA, should be introduced for the ON-state calculation, to be consistently connected with the classical boundary conditions described in Section II-B. The asymmetric distribution function with respect to $k = 0$ in the source region of Fig. 6(b) represents that the large drain current is flowing through the device at the ON-state.

C. I_D–V_G Characteristics

Next, we present current–voltage characteristics of SNWTs and discuss a scaling limit. Fig. 7 shows the I_D–V_G characteristics for $L_G = 9$, 6, and 4.5 nm, computed by using the Wigner and Boltzmann approaches. In the Wigner approach, a perceptible increase of the subthreshold current is obtained for the gate length shorter than 6 nm [15], which is due to the S-D tunneling as previously described. We note that band-to-band tunneling is not considered here, because the drain bias is sufficiently smaller than the effective bandgap energy of Si nanowire, including quantized energies. On the other hand, at higher V_G conditions, the two approaches become closer because thermal injection is a dominant carrier-injection process at the ON-state. Furthermore, the SSs are calculated,

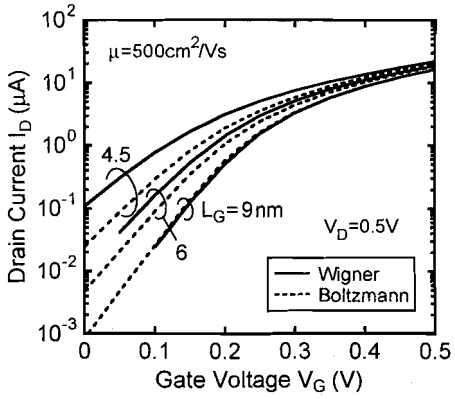

Fig. 7. I_D–V_G characteristics for $L_G = 9$, 6, and 4.5 nm, computed by using the Wigner and Boltzmann approaches.

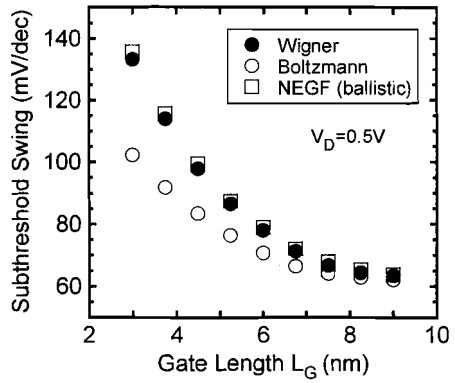

Fig. 8. Gate-length dependences of SSs computed by using the Wigner, Boltzmann, and ballistic NEGF approaches.

and the results are compared with those from the ballistic NEGF method [8], as shown in Fig. 8, where we also developed the ballistic NEGF source code in this study. It is found that the Wigner and ballistic NEGF results coincide closely for a wide range of gate length shorter than 10 nm. In this paper, to demonstrate how reasonable the comparison of SS values with the ballistic NEGF approach, we investigated the effect of carrier scattering on the I_D–V_G characteristics for the Wigner and Boltzmann approaches, as shown in Fig. 9, where the mobility was varied as 100, 250, and 2500 $\mathrm{cm}^2/(\mathrm{V}\cdot\mathrm{s})$. As a matter of course, the drain current decreases for the smaller mobility. However, it should be noted that SS values are barely affected by the value of the mobility, i.e., carrier scattering. Recently, the similar results have been reported within RTA based on the semiclassical Boltzmann approach [2]. Consequently, the comparison of SS values with the ballistic NEGF approach, as shown in Fig. 8, is considered to be valid.

Here, it is noteworthy that the I_D–V_G characteristics of the Wigner approach becomes closer to those of the semiclassical Boltzmann approach as the mobility (i.e., relaxation time) decreases, as shown in Fig. 9. This represents that when the coherency of electron waves is lost by the carrier scattering, the semiclassical carrier transport is recaptured in the Wigner transport equation [13]. This is an interesting and unique feature of the Wigner transport theory.

Furthermore, from Fig. 8, we can identify an influence of S-D tunneling on SS values. Indeed, we find that the semiclassical Boltzmann simulations without S-D tunneling might predict about 1-nm-shorter minimum gate length, enabling us to make electrostatically "well-tempered" GAA-SNWTs with an SS less than 80 mV/dec [3]. This discrepancy will not be negligible in practical design of SNWTs with sub-10 nm gate length.

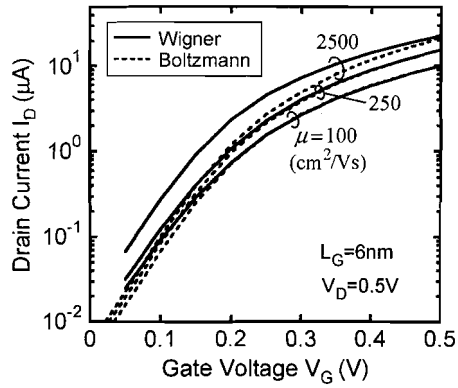

Fig. 9. Effect of carrier scattering on I_D–V_G characteristics, where the mobility was given by 100, 250, and 2500 $\mathrm{cm}^2/(\mathrm{V}\cdot\mathrm{s})$. Both of the Wigner and Boltzmann results are plotted. $L_G = 6$ nm and $V_D = 0.5$ V.

Finally, we describe a subject for future investigation regarding the Wigner function model. As shown in Fig. 7, the present Wigner approach cannot adequately compute electrical characteristics below certain current level, particularly for the longer channel devices. This is due to insufficient numerical accuracy under the conditions leading to higher and wider potential barriers [14]. For more reliable off-current simulation, we need to develop more advanced computational techniques, such as accurate discretization methodology and a proper connection with the correlated boundary conditions.

IV. Conclusion

We presented a 3-D quantum simulator for SNWTs based on the Wigner function model, which can consider 3-D electrostatic gate control, 2-D quantum confinement, and S-D tunneling. First, we demonstrated that the higher order differencing scheme is needed to achieve a sufficient numerical accuracy in the subthreshold region. The validity of the simulator was confirmed by comparing with the semiclassical Boltzmann and NEGF approaches. We also demonstrated that the influence of S-D tunneling begins to appear notably as the gate length becomes shorter than 6 nm and also that the semiclassical Boltzmann simulation without the S-D tunneling measurably underestimates a minimum gate length. We further pointed out that some advancement in the computational techniques is required to apply the Wigner function model to the off-current analysis.

References

[1] N. Neophytou, A. Paul, M. Lundstrom, and G. Klimeck, "Bandstructure effects in silicon nanowire electron transport," *IEEE Trans. Electron Devices*, vol. 55, no. 6, pp. 1286–1297, Jun. 2008.

[2] S. Scaldaferri, G. Curatola, and G. Iannaccone, "Direct solution of the Boltzmann transport equation and Poisson–Schrödinger equation for nanoscale MOSFETs," *IEEE Trans. Electron Devices*, vol. 54, no. 11, pp. 2901–2909, Nov. 2007.

[3] S. Jin, T.-W. Tang, and M. V. Fischetti, "Simulation of silicon nanowire transistors using Boltzmann transport equation under relaxation time approximation," *IEEE Trans. Electron Devices*, vol. 55, no. 3, pp. 727–736, Mar. 2008.
[4] M. Lenzi, P. Palestri, E. Gnani, S. Reggiani, A. Gnudi, D. Esseni, L. Selmi, and G. Baccarani, "Investigation of the transport properties of silicon nanowires using deterministic and Monte Carlo approaches to the solution of the Boltzmann transport equation," *IEEE Trans. Electron Devices*, vol. 55, no. 8, pp. 2086–2096, Aug. 2008.
[5] S. Jin, Y. J. Park, and H. S. Min, "A three-dimensional simulation of quantum transport in silicon nanowire transistor in the presence of electron–phonon interactions," *J. Appl. Phys.*, vol. 99, no. 12, p. 123 719, Jun. 2006.
[6] W. R. Frensley, "Wigner-function model of a resonant-tunneling semiconductor device," *Phys. Rev. B, Condens. Matter*, vol. 36, no. 3, pp. 1570–1580, Jul. 1987.
[7] H. Tsuchiya, M. Ogawa, and T. Miyoshi, "Simulation of quantum transport in quantum devices with spatially varying effective mass," *IEEE Trans. Electron Devices*, vol. 38, no. 6, pp. 1246–1252, Jun. 1991.
[8] S. Datta, *Electronic Transport in Mesoscopic Systems*. Cambridge, U.K.: Cambridge Univ. Press, 1995.
[9] H. Tsuchiya and T. Miyoshi, "Nonequilibrium Green's function approach to high-temperature quantum transport in nanostructure devices," *J. Appl. Phys.*, vol. 83, no. 5, pp. 2574–2585, Mar. 1998.
[10] C. Jacoboni and P. Bordone, "The Wigner-function approach to non-equilibrium electron transport," *Rep. Prog. Phys.*, vol. 67, no. 7, pp. 1033–1071, Jul. 2004.
[11] W. R. Frensley, "Boundary conditions for open quantum systems driven far from equilibrium," *Rev. Mod. Phys.*, vol. 62, no. 3, pp. 745–791, Jul. 1990.
[12] F. A. Buot and K. L. Jensen, "Lattice Weyl–Wigner formulation of exact many-body quantum-transport theory and application to novel solid-state quantum-based device," *Phys. Rev. B, Condens. Matter*, vol. 42, no. 15, pp. 9429–9457, Nov. 1990.
[13] H. Tsuchiya, M. Ogawa, and T. Miyoshi, "Quantum-mechanical simulation of electron waveguides in linear and nonlinear transport regimes," *IEEE Trans. Electron Devices*, vol. 39, no. 11, pp. 2465–2471, Nov. 1992.
[14] R. K. Mains and G. I. Haddad, "An accurate re-formulation of the Wigner function method for quantum transport modeling," *J. Comput. Phys.*, vol. 112, no. 1, pp. 149–161, May 1994.
[15] D. Querlioz, J. Saint-Martin, K. Huet, A. Bournel, V. Aubry-Fortuna, C. Chassat, S. Galdin-Retailleau, and P. Dollfus, "On the ability of the particle Monte Carlo technique to include quantum effects in nano-MOSFET simulation," *IEEE Trans. Electron Devices*, vol. 54, no. 9, pp. 2232–2242, Sep. 2007.

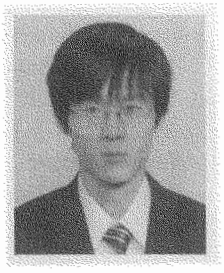

Yoshihiro Yamada was born in Kanagawa, Japan, on June 7, 1983. He received the B.S. and M.S. degrees in electrical and electronics engineering from Kobe University, Kobe, Japan, in 2006 and 2008, respectively, where he is currently working toward the Ph.D. degree in the Department of Electrical and Electronics Engineering, Graduate School of Engineering.

His research involves quantum-transport modeling of nanowire devices and first principles simulation of atomic-scale devices.

Mr. Yamada is a member of the Japan Society of Applied Physics.

Hideaki Tsuchiya (M'93–SM'01) was born in Ehime, Japan, on August 12, 1964. He received the B.S., M.S., and Ph.D. degrees in electronic engineering from Kobe University, Kobe, Japan, in 1987, 1989, and 1993, respectively.

In 1993, he was a Research Associate with the Department of Electrical and Electronics Engineering, Kobe University. He has been engaged in research of quantum-transport simulation of mesoscopic devices. From 1999 to 2000, he was a Visiting Scientist at the University of Illinois at Urbana–Champaign, Urbana. Since 2003, he has been an Associate Professor with the Department of Electrical and Electronics Engineering, Graduate School of Engineering, Kobe University. His current research includes the quantum-transport modeling of nanoscale MOSFETs and the first principles simulation of atomic-scale devices.

Dr. Tsuchiya is a member of the Institute of Electronics, Information and Communication Engineers of Japan and the Japan Society of Applied Physics. He was the recipient of the Young Scientist Award in 1998 from the Japan Society of Applied Physics and the Outstanding Achievement Award for a pioneering research on nanoscale device simulator in 2006 from the Institute of Electronics, Information and Communication Engineers of Japan.

Matsuto Ogawa (S'82–M'85) received the B.E. degree in electrical engineering and the M.S. and Ph.D. degrees in electronic engineering from the University of Tokyo, Tokyo, Japan, in 1980, 1982, and 1985, respectively.

In 1985, he became a Research Associate with the Department of Electronic Engineering, Kobe University, Kobe, Japan, where he is currently a Full Professor. He has been engaged in research of lightwave electronics and nanoscaled devices. His current research includes quantum-transport modeling in nanostructures. From 1992 to the end of 1993, he was on leave with IBM T. J. Watson Research Center, NY, as a Visiting Scientist.

Dr. Ogawa is a member of the Japan Society of Applied Physics and the Institute of Electronics, Information and Communication Engineers (IEICE) of Japan. He was the recipient of the Electronics Society Award in 2006 from the IEICE and the Project Research Award from the Semiconductor Technology Academic Research Center in 2008.